Simulation of Desulfurization in a Fluidized-Bed Limestone Reactor

Tho-Ching Ho, Hom-Ti Lee, J. R. Hopper
Department of Chemical Engineering
Lamar University
Beaumont, TX 77710

One of the most promising techniques of sulfur dioxide removal from flue gas is sorption using a fluidized bed of limestone. Two commonly considered schemes are the passing of combustion gases through the fluidized bed of limestone or actually burning fuel, e.g., coal, within such a bed (Zielke et al., 1970). Although the latter alternative seems to be more attractive and has been under intensive investigation (Horio and Wen, 1976; Zheng et al., 1982) the former scheme is also desirable since it can be designed to operate in conjunction with existing combustors. Recently, Wormser Engineering, Inc. (Kaplan, 1982) has developed a two-stage fluidized-bed coal combustor with the bottom stage being the coal combustor and the upper stage the limestone desulfurization reactor. The design appears to provide easier temperature control and better desulfurization efficiency compared to a single-stage, fluidized-bed coal-limestone combustor.

The objective of this study was to model and simulate a fluidized-bed limestone desulfurization reactor by coupling a grain model for reaction kinetics with a fluidized-bed model based on the two-phase theory. The stack gas from a combustor containing sulfur dioxide was used as the fluidizing gas. The effects of the gas and solid flow rates, bed height, limestone properties, and operating temperature on the desulfurization efficiency were investigated.

Mechanism

The mechanism of the desulfurization reaction involves two consecutive steps, calcination of calcium carbonate followed by reaction of calcium oxide with sulfur dioxide, i.e.,

$$CaCO_{3(s)} \rightleftharpoons CaO_{(s)} + CO_{2(g)} \qquad [I]$$

and

$$CaO_{(s)} + SO_{2(g)} + \frac{1}{2} O_{2(g)} \rightarrow CaSO_{4(s)} \qquad [II]$$

It has been observed that reaction I is usually fast at high temperature; however, reaction II decreases its reaction rate rapidly as sulfation proceeds.

Mathematical Formulation

The simulation model developed in this study included a grain model and a fluidized-bed model. The grain model is useful for analysis of a reaction involving a gas reactant and porous particles. It generates the conversion data with respect to reaction time within a particle. The grain model used is essentially the one proposed by Hartman and Coughlin (1976) and is not described here.

Fluidized-bed model

The fluidized-bed model proposed is based on the two-phase theory and is designed for large particle systems ($d_p > 1$ mm). The model has the following assumptions:

1. The bed is composed of two phases, the bubble and the emulsion phases.
2. The volumetric flux through the bubble phase is constant throughout the bed, and the rest of the gas flows through the emulsion phase.
3. The gaseous reactant disappears according to a first-order reaction

$$-\frac{1}{V_{\text{solid}}}\frac{dN_A}{dt} = K_r C_A \qquad (1)$$

Based on these assumptions, steady state material balances on the gaseous reactant A in the bubble phase and emulsion phase have the following forms:

$$\frac{dC_{Ab}}{dl} = -\frac{\delta}{V_B} K_{be}(C_{Ab} - C_{Ae}) \qquad (2)$$

and

$$\frac{dC_{Ae}}{dl} = \frac{\delta}{U - V_B}\left[K_{be}(C_{Ab} - C_{Ae}) - \frac{(1-\delta)(1-\epsilon_{mf})}{\delta} K_r C_{Ae}\right] \quad (3)$$

with boundary conditions

$$C_{Ab} = C_{Ae} = C_{A,O} \quad \text{at } l = 0 \quad (4)$$

The parameters appearing in the above equations are evaluated by the following equations:

1. The bed fraction of bubble phase, δ, is determined by

$$\delta = 1 - \frac{L_{mf}}{L_f} \quad (5)$$

where, L_f/L_{mf} is given by (Babu et al., 1978)

$$\frac{L_f}{L_{mf}} = 1 + \frac{1.9544(U - U_{mf})^{0.738} d_p^{1.006} \rho_p^{0.736}}{U_{mf}^{0.937} \rho_g^{0.126}} \quad (6)$$

2. The average volumetric flux of gas through the bubble phase, V_B, is determined by (Cranfield and Geldart, 1974)

$$V_B = 0.333\,(U - U_{mf})^{1.11} L_f^{1.09} \quad (7)$$

3. The minumum fluidization velocity, U_{mf}, is evaluated by (Wen and Yu, 1966)

$$\frac{d_p U_{mf} \rho_g}{\mu} = \left[(33.7)^2 + 0.0408 \frac{d_p^3 \rho_g (\rho_p - \rho_g) g}{\mu^2}\right]^{0.5} - 33.7 \quad (8)$$

4. The average bubble size of the bed, d_b, is calculated by (Mori and Wen, 1975)

$$d_b = d_{bM} - \frac{(d_{bM} - d_{bO}) D_t}{0.3 L_f}\left[1 - \exp\left(\frac{-0.3 L_f}{D_t}\right)\right] \quad (9)$$

where

$$d_{bm} = 0.652\,[A_t(U - U_{mf})]^{0.4} \quad (10)$$

and

$$d_{bO} = 0.347\,[(U - U_{mf})/n_d]^{0.4} \quad (11)$$

5. The gas interchange coefficient, K_{be}, is determined by (Davidson and Harrison, 1963)

$$K_{be} = 4.5\left(\frac{U_{mf}}{d_b}\right) + 5.85\left(\frac{D_b^{0.5} g^{0.25}}{d_b^{1.25}}\right) \quad (12)$$

Given a reaction rate constant, K_r, the gas concentrations in the bubble and emulsion phases, C_{Ab} and C_{Ae}, can be solved numerically from Eqs. 2 and 3 coupling with Eqs. 5–12. The mean concentration of the gaseous reactant A in the emulsion phase and in the exit gas stream are then calculated by

$$\bar{C}_{Ae} = \frac{1}{L_f}\int_0^{L_f} C_{Ae}\, dl \quad (13)$$

and

$$\bar{C}_{A,f} = \frac{U - V_B}{U} C_{Ae,f} + \frac{V_B}{U} C_{Ab,f} \quad (14)$$

The overall conversion of the gas reactant is then evaluated by

$$X_{A,f} = 1 - \frac{\bar{C}_{A,f}}{C_{A,O}} \quad (15)$$

It is worth pointing out that if the reaction rate constant K_r appearing in Eq. 3 is a known value, the fluidized-bed model described above is sufficient to give a complete description of the reactor performance. However, since the desulfurization reaction between limestone and sulfur dioxide is complex, a sophisticated kinetic model such as a grain model is required.

Simulation model

Figure 1 shows a fluidized-bed limestone desulfurization reactor under consideration. In addition to the assumptions stated previously, the following assumptions were made in the simulation:

1. The reactor is under steady state operation.
2. The limestone particles are of uniform size and are completely mixed in the bed.
3. No elutriation of particles occurs.

Following these assumptions, an iterative computational scheme was proposed that treated the reaction rate constant K_r

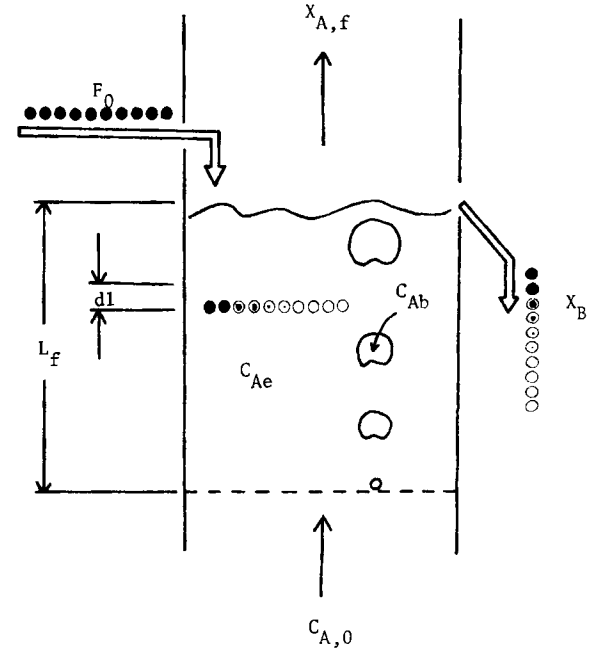

Figure 1. Diagram of fluidized-bed desulfurization reactor.

Table 1. Typical Sets of Input Data

Variable	Set 1	Set 2	Set 3	Set 4	Set 5	Set 6	Set 7	Set 8
	Stone*							
	a	a	a	a	b	b	b	c
e_{LS}	0.0	0.0	0.0	0.0	0.1	0.1	0.1	0.0
ρ_{LS}	2.71	2.71	2.71	2.71	2.86	2.86	2.86	2.78
y_{CC}	0.982	0.982	0.982	0.982	0.555	0.555	0.555	0.680
y_{MC}	0.0	0.0	0.0	0.0	0.344	0.344	0.344	0.04
X_C	1.0	1.0	1.0	1.0	1.0	1.0	1.0	0.89
e_c	0.52	0.52	0.52	0.52	0.56	0.56	0.56	0.315
$r_g \times 10^5$ cm	1.0	1.0	1.0	1.0	2.0	1.0	0.6	2.0
T, K	1123	1123	1123	1088	923	1033	1143	1088
d_p, cm	0.0565	0.09	0.112	0.1095	0.0096	0.0096	0.0096	0.1095
$C_O \times 10^8$ mol/cm^3	3.2	3.2	3.2	5.6	2.9	2.9	2.9	5.6

*a, Limestone VI (Hartman and Couglin, 1974, 1976).
b, Dolomite 1351 (Borgwardt, 1970).
c, Greer limestone (Ulerich, 1977).

in Eq. 3 as a parameter. The calculation procedures are described below.

1. Input data. Typical sets of input data are summarized in Table 1.

2. Assume initial value for K_r.

3. Calculate $X_{A,f}$ and C_{Ae} from the fluidized-bed model, i.e., solving Eqs. 2–15 using the Runge-Kutta method.

4. Apply the grain model to determine the conversion of limestone particle X_B as a function of residence time t with $\bar{C}_{Ae}$ calculated in step 3 being the bulk concentration of SO_2.

5. Determine the mean conversion of the limestone in the limestone exit stream, $\bar{X}_B$, by

$$\bar{X}_B = \int_{t=0}^{\infty} X_B(t)E(t)\,dt \tag{16}$$

Notice that the residence time distribution of the particles, $E(t)$, is given by

$$E(t) = \frac{1}{\bar{t}} e^{-t/\bar{t}} \tag{17}$$

according to assumption 2, and $\bar{t}$ is expressed as

$$\bar{t} = \frac{W}{F_0} = \frac{L_{mf}A_t(1-\epsilon_{mf})\rho_{LS}}{F_0} \tag{18}$$

6. Estimate the overall conversion of SO_2, $X'_{A,f}$, from $\bar{X}_B$ using the following material balance equation

$$\frac{F_0 y_{CC} X_C}{M_{CO}} \bar{X}_B = UA_t C_{A,O} X'_{A,f} \tag{19}$$

7. Compare $X_{A,f}$ calculated from step 3 with $X'_{A,f}$ calculated from step 6. If they are not identical, determine a new trial value for K_r using Muller's method (Gerald, 1978) and repeat steps 2 through 7.

8. Stop when $X_{A,f}$ and $X'_{A,f}$ are identical. The criterion used was $|X_{A,f} - X'_{A,f}| < 10^{-3}$.

Results and Discussion

Figure 2 shows a typical set of the simulation results where the effects of SO_2 concentration and the U/U_{mf} ratio on the desulfurization efficiency, $X_{A,f}$, are presented. The figure indicates that the desulfurization efficiency is lower at higher U/U_{mf}

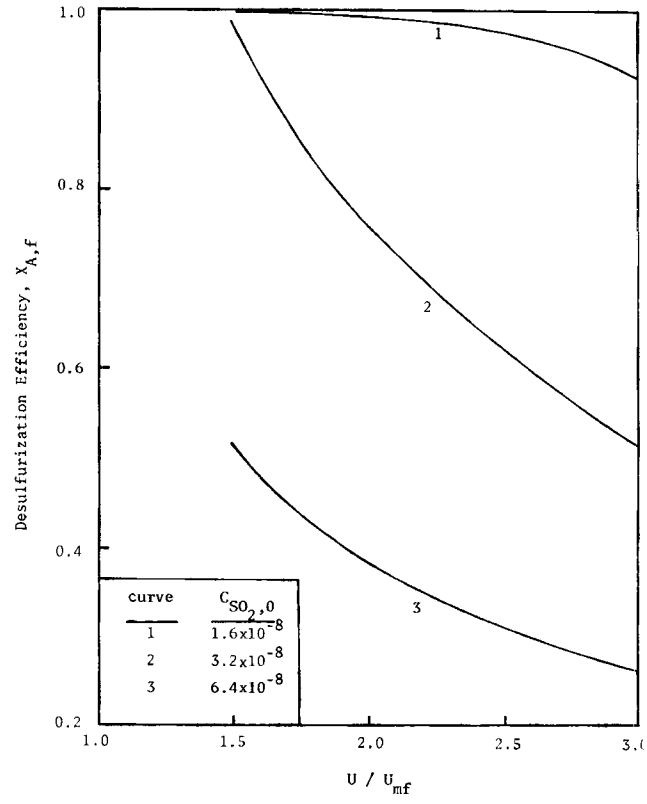

Figure 2. Effect of inlet SO_2 concentration on desulfurization efficiency at various U/U_{mf} ratios.
Limestone VI. d_p = 0.1205 cm; T = 1,123 K; U_{mf} = 48.88 cm/s; L_{mf} = 30 cm; t = 20 h; D_t = 50 cm; n_d = 1.5.

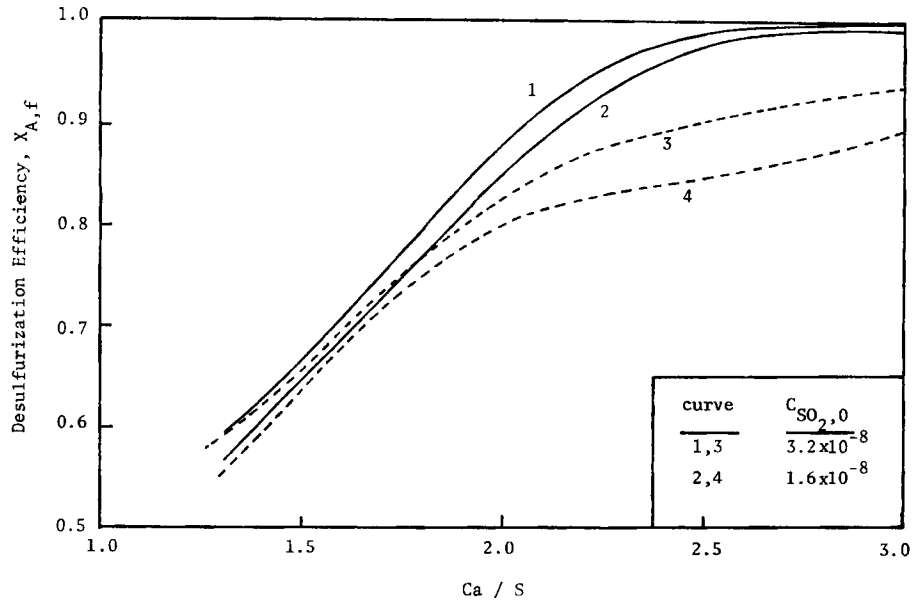

Figure 3. Effect of inlet SO_2 concentration on desulfurization efficiency at various Ca/S ratios.
Limestone VI. d_p = 0.1205 cm; T = 1,123 K; U/U_{mf} = 2.0; L_{mf} = 30 cm; D_t = 50 cm; n_d = 1.5.
Curves 1, 2: two-phase model; curves 3, 4: stirred-tank model.

and higher inlet SO_2 concentration. The results shown are expected since it contains more SO_2 at higher U/U_{mf} and higher $C_{SO_2,O}$. The higher SO_2 content causes the Ca/S ratio to drop, which in turn causes the desulfurization efficiency to decrease. It has been discovered through this study and other previous studies (Horio and Wen, 1976; Zheng et al., 1982) that the Ca/S ratio is the most critical parameter governing the reactor performance. Once the Ca/S ratio is fixed, the other parameters, such as T, $C_{SO_2,O}$, d_p, and other limestone properties, affect the desulfurization efficiency only moderately or slightly. Notice that the Ca/S ratio is a function of $C_{SO_2,O}$, U, F_o, and the limestone properties. It can be formulated as

$$\frac{\text{Ca}}{\text{S}} = \frac{\text{mol Ca}}{\text{mol S}} = \frac{L_{mf}(1-\epsilon_{mf})\rho_{LS}y_{CC}}{M_{CC}\bar{t}C_{SO_2,O}U} \tag{20}$$

The variations in the desulfurization efficiency as a function of Ca/S ratio are shown in Figures 3 through 5.

Figure 3 plots the desulfurization efficiency vs. the Ca/S ratio with $C_{SO_2,O}$ as the parameter. The results from this figure indicate that, at the same Ca/S ratio, the inlet SO_2 concentration affects the efficiency only slightly; a higher concentration

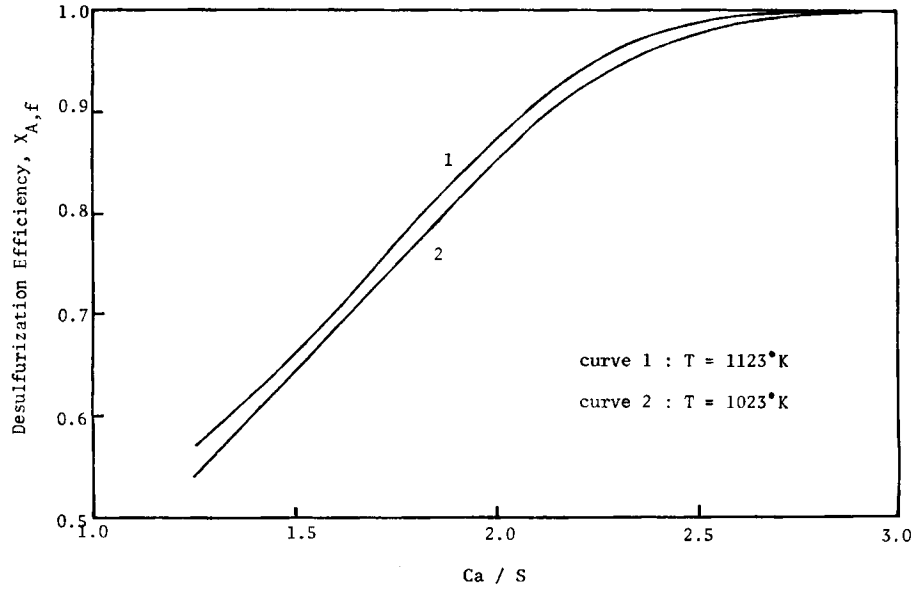

Figure 4. Effect of temperature on desulfurization efficiency at various Ca/S ratios.
Limestone VI. d_p = 0.1205 cm; $C_{SO_2,O} = 3.2 \times 10^{-8}$ mol/cm^3; U/U_{mf} = 2.0; L_{mf} = 30 cm; D_t = 50 cm; n_d = 1.5.

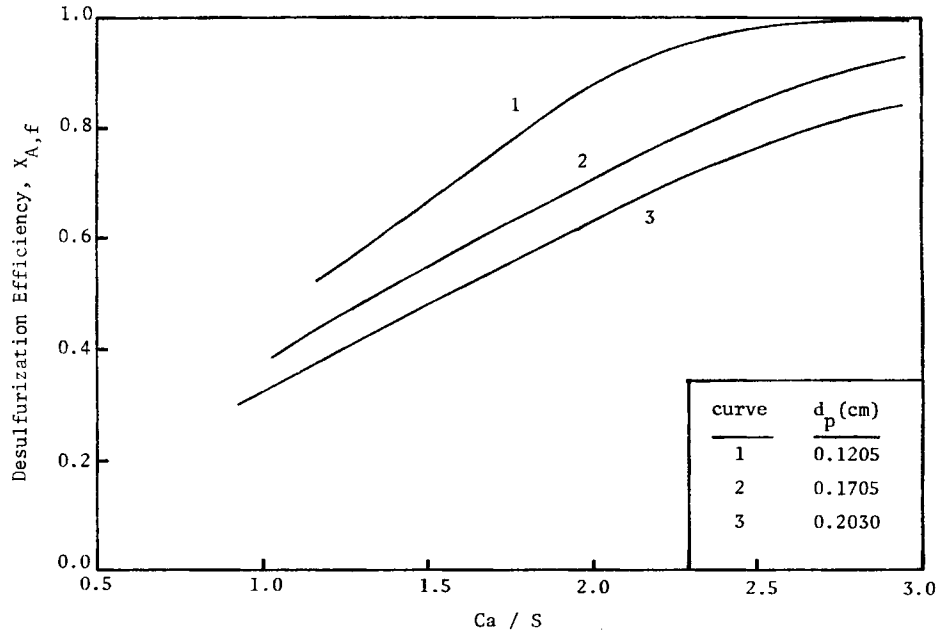

Figure 5. Effect of particle size on desulfurization efficiency at various Ca/S ratios.
Limestone VI. T = 1,123 K; $C_{SO_2,O} = 3.2 \times 10^{-8}$ mol/cm^3; U/U_{mf} = 2.0; L_{mf} = 30 cm; D_t = 50 cm; n_d = 1.5.

corresponds to a higher efficiency. Also plotted on the figure are results from a mixed-tank model. As indicated, the two models, i.e., two-phase model and mixed-tank model, essentially predict the same results at low to medium Ca/S ratios. The mixed-tank model, however, predicts lower desulfurization efficiency at relatively high Ca/S ratios. Figure 4 shows the effect of operating temperature on the desulfurization efficiency under a fixed Ca/S condition. These results indicate that temperature affects the efficiency only slightly. The results show that the efficiency reaches 80% at Ca/S = 1.9. The effect of limestone size on the desulfurization efficiency is shown in Figure 5. As indicated in the figure, the particle size has a moderate effect on the efficiency; a smaller particle size gives a better desulfurization efficiency. The two types of limestone used in this simulation have little effect on the desulfurization efficiency, as can be seen in Figure 6.

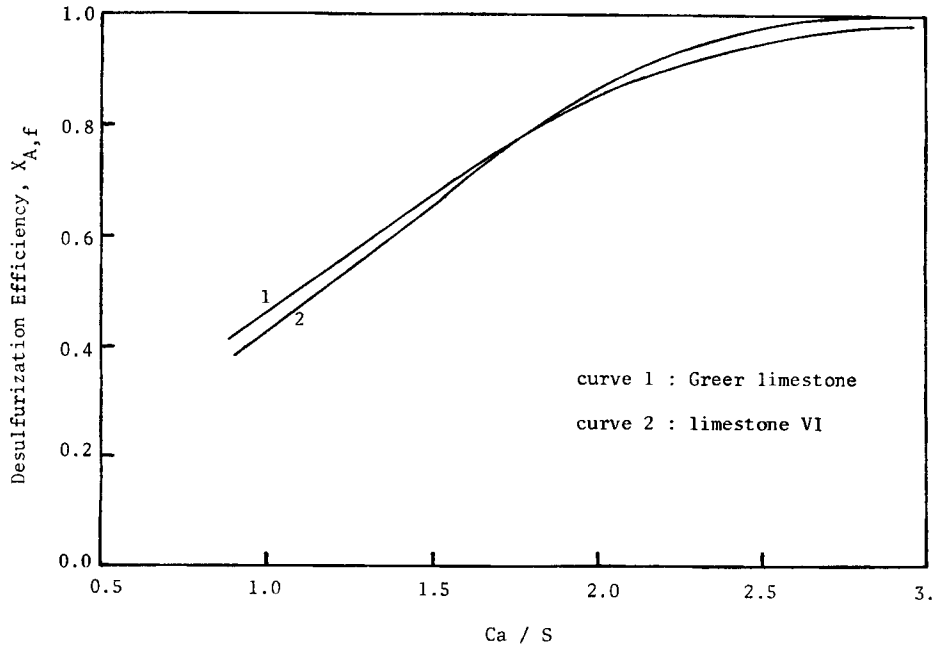

Figure 6. Comparison of desulfurization efficiency of limestone VI and Greer limestone.
d_p = 0.1205 cm; T = 1,123 K; $C_{SO_2,O} = 3.2 \times 10^{-8}$ mol/cm^3; U/U_{mf} = 2.0; L_{mf} = 30 cm; n_d = 1.5.

Although it is not shown in the figures, it has been found that the reactor hydrodynamics, e.g., bed height, bubble size, and number of holes in the distributor, have little effect on the desulfurization efficiency. This is due to the fact that the desulfurization reaction is a slow reaction (Fogler and Brown, 1981). It is worth pointing out that the EPA standard for new coal-fired plants of 1.2 lb SO_2/MBtu (0.54 kg/MJ) of fuel burned, which corresponds to about 81% desulfurization for a 3.5% sulfur coal, can easily be met in a fluidized-bed limestone desulfurization reactor, as indicated in the simulation results.

Notation

A_t = cross-sectional area of bed, cm^2
C_A = concentration of reactant gas A in the bed, mol/cm^3
C_{Ab} = concentration of reactant gas A in gas bubble, at a given level in bed, mol/cm^3
C_{Ae} = concentration of reactant gas A in emulsion phase at a given level in bed, mol/cm^3
$C_{A,O}$ = concentration of reactant gas A in entering gas stream, mol/cm^3
$C_{Ab,f}$ = exit gas concentration from bubble phase, mol/cm^3
$C_{Ae,f}$ = exit gas concentration from emulsion phase, mol/cm^3
C_{Ae} = mean concentration of reactant gas A in emulsion phase, mol/cm^3
$\bar{C}_{A,f}$ = mean concentration of reactant gas A in exit gas stream, mol/cm^3
$C_{SO_2,O}$ = concentration of SO_2 in entering gas stream, mol/cm^3
C_0 = concentration of reactant gas outside spherical particle, mol/cm^3
D_b = molecular diffusion coefficient of gas, cm^2/s
D_t = diameter of the fluidized bed, cm
d_b = average bubble dia., cm
d_{bO} = initial bubble dia. at distributor, cm
d_{bM} = maximum bubble dia. due to total coalescences of bubbles, cm cm
d_p = dia. of particle, cm
$E(t)$ = exit age distribution function, s^{-1}
e_c = porosity of calcined limestone
e_{LS} = porosity of raw limestone
F_O = feed rate of solids, g/cm
g = gravitational acceleration, cm/s^2
K_{be} = overall coefficient of gas interchange between bubble phase and emulsion phase based on volume of bubbles, s^{-1}
K_r = reaction rate constant in Eq. 3, s^{-1}
L_f = expanded bed height, cm
L_{mf} = bed height at minimum fluidizing conditions, cm
l = elevation above the distributor, cm
M_{CC} = molecular weight of C_aCO_3, g/mol
M_{CO} = molecular weight of CaO, g/mol
N_A = moles of reactant A
n_d = number of holes per unit area of perforated distributor, holes/cm^2
r_g = radius of grain, cm
T = temperature, K
t = time, s
$\bar{t}$ = mean residence time of solids in the bed, s
U = superficial gas velocity (measured on an empty bed basis) through a bed of solids, cm/s
U_{mf} = superficial gas velocity at minimum fluidizing conditions, cm/s
V_{solid} = solid volume, cm^3
V_B = volumetric flux through bubble phase, $cm^3/cm^2 \cdot s$
W = total weight of solids in bed, g
$X_{A,f}$ = overall conversion of reactant gas A in exit gas stream
$X_B(t)$ = conversion of CaO with residence time between t and $t + dt$
$\bar{X}_B$ = mean conversion of CaO in limestone exit stream
X_C = total fraction of $CaCO_3$ converted to CaO and $CaSO_4$
X_M = extent of calcination of $MgCO_3$
y_{CC} = content of $CaCO_3$ in limestone, weight fraction
y_{MC} = content of $MgCO_3$ in limestone, weight fraction

Greek Letters

δ = bed fraction of bubble phase
ϵ_{mf} = void fraction at minimum fluidizing conditions
μ = viscosity of fluidizing gas, $g/cm \cdot s$
ρ_g = density of fluidizing gas, g/cm^3
ρ_{LS} = true density of raw limestone, g/cm^3
ρ_p = true density of porous particle, g/cm^3

Literature cited

Babu, S. P., B. Shah, and A. Talwalkar, "Fluidization Correlations for Coal Gasification Materials—Minimum Fluidization Velocity and Fluidized Bed Expansion Ratio," *AIChE Symp. Ser.*, **74,** No. 176, 176 (1978).

Borgwardt, R. H., "Kinetics of the Reaction of SO_2 with Calcined Limestone," *Environ. Sci. Technol.*, **4,** 59 (1970).

Cranfield, R. R., and D. Geldart, "Large Particle Fluidization," *Chem. Eng. Sci.*, **29,** 935 (1974).

Davidson, J. F., and D. Harrison, *Fluidized Particle,* Cambridge Univ. Pr., New York, (1963).

Fogler, H. S. and L. F. Brown, "Predictions of Fluidized Bed Operation Under Two Limiting Conditions: Reaction Control and Transport Control," *Chemical Reactor,* H. S. Fogler, ed. Am. Chem. Soc. (1981).

Gerald, C. F., *Applied Numerical Analysis,* 2nd ed., Addison Wesley, (1978).

Hartman, M., and R. W. Coughlin, "Reaction of Sulfur Dioxide with Limestone and the Influence of Pore Structure," *Ind. Eng. Chem., Process Des. Dev.*, **13**(3), 248 (1974).

———, "Reaction of Sulfur Dioxide with Limestone and Grain Model," *AIChE J.*, **22**(3), 490 (1976).

Horio, M., and C. Y. Wen, "Analysis of Fluidized Bed Combustion of Coal with Limestone Injection," *Fluidization Technology,* Hemisphere, Washington, D.C., **2,** 289 (1976).

Kaplan, L., "Coal Combustor Retrofits to Gas- and Oil-Fired Boilers," *Chem. Eng.*, **89**(4), 54, (1982).

Mori, S., and C. Y. Wen, "Estimation of Bubble Diameter in Gaseous Fluidized Bed," *AIChE J.*, **21,** 109 (1975).

Ulerich, N. H., E. P. O'Neill, and D. L. Keairns, "The Influence of Limestone Calcination on the Utilization of the Sulfur Solvent in Atmospheric Pressure Fluid-Bed Combustors," EPRI-426, Final Report (1977).

Wen, C. Y., and Y. H. Yu, "A Generalized Method for Predicting the Minimum Fluidization Velocity," *AIChE J.*, **12,** 610 (1966).

Zheng, J., J. G. Yates, and P. N. Rowe, "A Model for Desulfurisation with Limestone in a Fluidized Coal Combustor," *Chem. Eng. Sci.*, **37,** 167 (1982).

Zielke, C. W., H. E. Lebowitz, R. T. Struck, and E. Gorin, "Sulfur Removal During Combustion of Solid Fuels in a Fluidized Bed of Dolomite," *Air Pollut. Control Assoc. J.*, **20,** 164 (1970).

Manuscript received Feb. 5, 1985, and revision received Dec. 26, 1985.